8. Passive Seismic Experiment

Gary V. Latham,[a†] *Maurice Ewing,*[a] *Frank Press,*[b]
George Sutton,[c] *James Dorman,*[a] *Yosio Nakamura,*[d] *Nafi Toksoz,*[b]
David Lammlein,[a] *and Fred Duennebier*[c]

With the successful installation of a geophysical station at Hadley Rille and the continued operation of the Apollo 12 and Apollo 14 stations approximately 1100 km southwest, the Apollo Program has for the first time achieved a network of seismic stations on the lunar surface, a network that is absolutely essential for the location of natural events on the Moon. The establishment of this network is one of the most important milestones in the geophysical exploration of the Moon.

Four major discoveries have resulted from the analysis of seismic data from this network for the 45-day period represented by this report.

(1) The Moon has a crust and a mantle, at least in the region of the Apollo 12 and Apollo 14 stations. The thickness of the crust is between 55 and 70 km and may consist of two layers. The contrast in elastic properties of the rocks that comprise the major structural units is at least as great as that existing between the crust and mantle of the Earth.

(2) Although present data do not permit a completely unambiguous interpretation, the best solution obtainable places the most active moonquake focus at a depth of 800 km, slightly deeper than any known earthquake. These moonquakes occur in monthly cycles and are triggered by lunar tides.

(3) In addition to the repeating moonquakes, moonquake "swarms" have been discovered. During periods of swarm activity, events may occur as frequently as one event every 2 hr during intervals lasting several days. The source of these swarms is unknown at present.

(4) Most of the seismic energy from a surface source is efficiently confined or trapped for a long time in the near-source region by efficient scattering near the lunar surface. The seismic energy slowly leaks to distant parts of the Moon, probably by more efficient seismic radiation within the lunar interior. Meteoroid impact signals are probably received from all parts of the Moon by efficient interior propagation.

The purpose of the passive seismic experiment (PSE) is to detect vibrations of the lunar surface and to use these data to determine the internal structure, physical state, and tectonic activity of the Moon. Sources of seismic energy may be internal (moonquakes) or external (meteoroid impacts and manmade impacts). A secondary objective of the experiment is the determination of the number and the masses of meteoroids that strike the lunar surface. The instrument is also capable of measuring tilts of the lunar surface and changes in gravity that occur at the PSE location.

Since deployment and activation of the Apollo 15 PSE on July 31, 1971, the instrument has operated as planned, except as noted in the following subsection entitled "Instrument Description and Performance." The sensor was installed west of the lunar module (LM) 110 m from the nearest LM footpad.

Signals were recorded from astronaut activities, particularly the movements of the lunar roving vehicle (Rover), at all points along the traverses (maximum range, approximately 5 km). The variation with range of Rover-generated seismic signals provides a measure of the amplitude decay law for seismic signals generated at close range.

The velocity of sound in the lunar regolith at the Apollo 15 landing site, as determined by timing the

[a]Lamont-Doherty Geological Observatory.
[b]Massachusetts Institute of Technology.
[c]University of Hawaii.
[d]General Dynamics.
[†]Principal investigator.

seismic signal generated by the LM ascent propulsion engine, is approximately 92 m/sec. This value is remarkably close to the regolith velocities of 104 and 108 m/sec measured at the Apollo 12 and Apollo 14 sites, respectively. The uniformity of the regolith velocities measured at widely separated sites indicates that the process of comminution by meteoroid impacts has produced a layer of remarkably uniform mechanical properties over the entire surface of the Moon.

Seismic signals from 75 events believed to be of natural origin were recorded by the long-period (LP) seismometers at one or more of the seismic stations during the 42-day period after the LM ascent. Of these events, at least two were moonquakes that originated in the region of greatest seismic activity, previously identified from recordings at the Apollo 12 and Apollo 14 stations; four were moonquakes from other locations; and 16 others were possible moonquakes. Of the remaining 53 events, 35 were probable meteoroid impacts, and 18 were too small or indistinct to be classified. The moonquakes occurred most frequently near the times of minimum (perigee) and maximum (apogee) distance between the Earth and the Moon during each monthly revolution of the Moon about the Earth, suggesting that the moonquakes are triggered by tidal stresses.

The A_1 epicenter (the point on the lunar surface directly above the moonquake source) is estimated to be nearly equidistant from the Apollo 12 and Apollo 14 sites and at a range of approximately 600 km south of the Apollo 12 station. Except for the absence of the surface-reflected phases usually seen on the records from deep earthquakes, the seismic data suggest that A_1 events, and perhaps all moonquakes, are deep. The best solution obtained to date places the A_1 moonquake focus at a depth of approximately 800 km. This depth is somewhat greater than that of any known earthquake. If this location is verified by future data, the result will have fundamental implications relative to the present state of the lunar interior. The nature of the stresses that might generate moonquakes at this depth is unknown at present. However, a secular accumulation of strain is inferred from the uniform polarity of the signals. In any case, if moonquakes originate at this depth, the deep lunar interior must possess sufficient shear strength to accumulate stress to the point of rupture. This condition places an upper bound on the temperatures that can exist at these depths.

A new method of data processing that enhances very small signals has revealed that episodes of greatly increased seismic activity occur. The events are very small and occur in some cases at average rates of one every 2 hr during intervals of several days. Individual events of these swarms appear to be moonquakes. Six such swarms occurred during April and May. These moonquake swarms do not appear to correlate with the monthly tidal cycle, as do the repeating moonquakes described previously. The locations and focal mechanisms of the sources of moonquake swarms are as yet unknown.

Seismic signals were recorded from two manmade impacts (the SIVB stage of the Saturn launch vehicle and the LM ascent stage) during the Apollo 15 mission. The LM-impact signal was the first event of precisely known location and time recorded by three instruments on the lunar surface. Data from these impacts combined with data from the impacts accomplished during the Apollo 12, 13, and 14 missions, and the lunar-surface magnetometer results are the main sources of information about the internal structure of the Moon. The general characteristics of the recorded seismic signals suggest that the outer shell of the Moon, to depths no greater than 20 km, is highly heterogeneous. The heterogeneity of the outer zone results in intensive scattering of seismic waves and greatly complicates the recorded signals. The structure of the scattering zone is not precisely known, but the presence of craters must contribute to the general complexity of the zone. The entire Moon is probably mantled by such a layer. The layered structure photographed at the Apollo 15 site suggests a sequence of thin lava flows. Each flow may have been highly fractured by thermal stresses while cooling and by meteoroid impacts before the overlying layer was deposited. A highly heterogeneous structure many kilometers thick may have been built up in this manner.

The LM ascent stage struck the surface 93 km west of the Apollo 15 station. The characteristic rumble from this impact spread slowly outward and was detected at the Apollo 15 station in approximately 22 sec, and at the Apollo 12 and Apollo 14 stations, 1100 km to the southwest, in approximately 7 min. The fact that this small source of energy was detected at such great range strongly supports the earlier hypothesis that the lunar interior, beneath the scattering zone, transmits seismic energy with extremely high efficiency. This observation strength-

ens the belief that meteoroid impacts are being detected from the entire lunar surface.

The Apollo 15 SIVB impact extended the depth of penetration of seismic rays to approximately 80 km. From these additional data, it now appears that a change in composition must occur at a depth of between 55 and 70 km. If so, this would be strong evidence of the presence of a lunar crust, analogous to the crust of the Earth and of about the same thickness. In the crustal zone, competent rock with a velocity for compressional waves of approximately 6 km/sec is reached at a depth of 15 to 20 km. The velocity begins to increase from 6 km/sec at a depth of between 20 and 25 km and reaches 9 km/sec at a depth of between 55 and 70 km. The presence of a secondary compressional-wave (P-wave) arrival suggests the possible existence of an intermediate layer that has a velocity of 7.5 km/sec. Thus, the lunar crust, in the region of the Apollo 12 and Apollo 14 stations, may consist of two layers: a surface layer with a velocity of 6 km/sec and a thickness of 20 to 25 km, overlying a layer with a thickness of between 30 and 50 km and a velocity of 7.5 km/sec, with a sharp increase in velocity to 9 km/sec at the base of the lower layer. Alternately, the transition from 6 to 9 km/sec may be gradual. Velocities between 6.7 and 6.9 km/sec are expected for the feldspar-rich rocks found at the surface. Thus, the measured velocities are within the range expected for these rocks.

The 9-km/sec material below a depth of 55 to 70 km may be the parent material from which the crustal rock has differentiated. If so, the Moon has undergone large-scale magmatic differentiation similar to that of the Earth.

INSTRUMENT DESCRIPTION AND PERFORMANCE

A seismometer consists simply of a mass that is free to move in one direction and that is suspended by means of a spring (or a combination of springs and hinges) from a framework. The suspended mass is provided with damping to suppress vibrations at the natural frequency of the system. The framework rests on the surface, the motions of which are to be studied, and moves with the surface. The suspended mass tends to remain fixed in space because of its own inertia, while the frame moves in relation to the mass. The resulting relative motion between the mass and the framework can be recorded and used to calculate original ground motion if the instrumental constants are known.

The Apollo 15 PSE consists of two main subsystems: the sensor unit and the electronics module. The sensor unit, shown schematically in figure 8-1, contains three matched LP seismometers (with resonant periods of 15 sec) alined orthogonally to measure one vertical (Z) and two horizontal (X and Y) components of surface motion. The sensor unit also includes a single-axis short-period (SP) seismometer (with a resonant period of 1 sec) that is sensitive to vertical motion at higher frequencies. The instrument is constructed principally of beryllium and weighs 11.5 kg, including the electronics module and thermal insulation. Without insulation, the sensor unit is 23 cm in diameter and 29 cm high. The total power drain varies between 4.3 and 7.4 W.

Instrument temperature control is provided by a 6-W heater, a proportional controller, and an aluminized Mylar insulation. The insulating shroud is spread over the local surface to reduce temperature variations of the surface material.

The LP seismometer detects vibrations of the lunar surface in the frequency range from 0.004 to 2 Hz. The SP seismometer covers the band from 0.05 to 20 Hz. The LP seismometers can detect ground motions as small as 0.3 nm at maximum sensitivity in the flat-response mode; the SP seismometer can detect ground motions of 0.3 nm at 1 Hz.

The LP horizontal-component (LPX and LPY) seismometers are very sensitive to tilt and must be leveled to high accuracy. In the Apollo system, the seismometers are leveled by means of a two-axis, motor-driven gimbal. A third motor adjusts the LP vertical-component (LPZ) seismometer in the vertical direction. Motor operation is controlled by command. Calibration of the complete system is accomplished by applying an accurate increment or step of current to the coil of each of the four seismometers by transmission of a command from Earth. The current step is equivalent to a known step of ground acceleration.

A caging system is provided to secure all critical elements of the instrument against damage during the transport and deployment phases of the Apollo mission. In the present design, a pneumatic system is used in which pressurized bellows expand to clamp fragile parts in place. Uncaging is performed on command by piercing the connecting line by means of a small explosive device.

was generated by the thrust of the LM ascent engine.

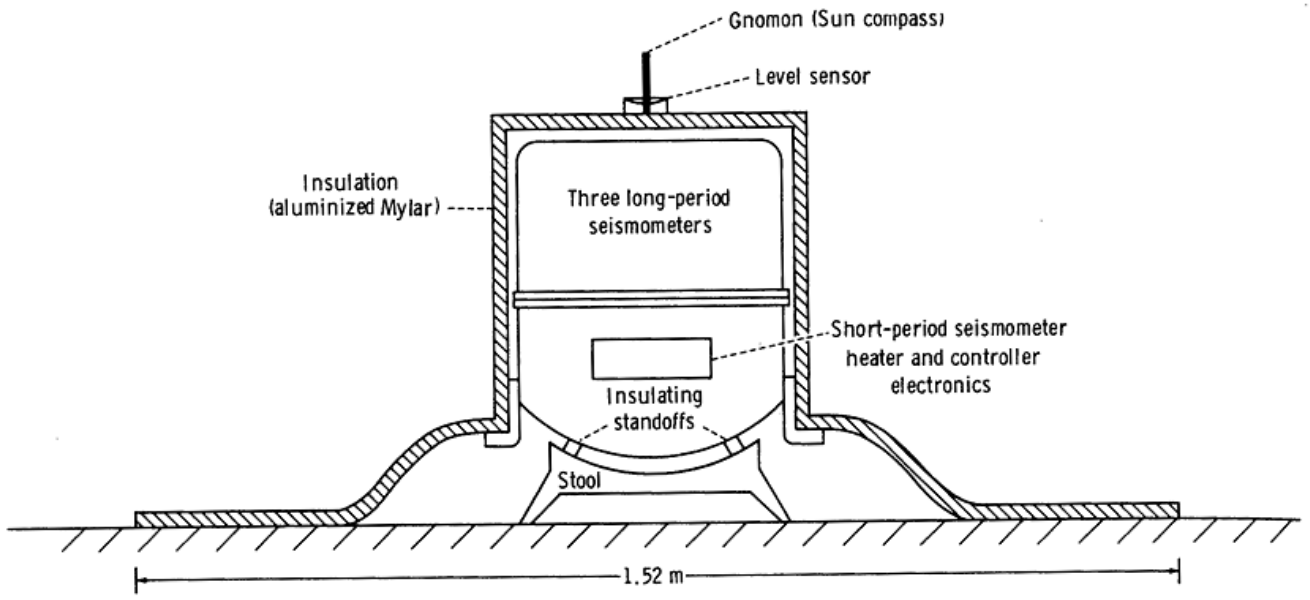

FIGURE 8-1.–Schematic diagram of PSE.

The seismometer system is controlled from Earth by a set of 15 commands that govern functions such as speed and direction of leveling motors, and instrument gain and calibration. In figure 8-2, the seismometer is shown fully deployed on the lunar surface.

Two modes of operation of the LP seismometers are possible: the flat-response mode and the peaked-response mode. In the flat-response mode, the seismometers have natural periods of 15 sec. In the peaked-response mode, the seismometers act as underdamped pendulums with natural periods of 2.2 sec. Maximum sensitivity is increased by a factor of 6 in the peaked-response mode, but sensitivity to low-frequency signals is reduced. The response curves for both modes are shown in figure 8-3.

The PSE was deployed 3 m west of the central station. No difficulty was experienced in deploying the experiment. Since initial activation of the PSE, all elements have operated as planned, with the exception of the sensor thermal-control system. The sensor temperature fell below the design setpoint of 126° F to a minimum of 112° F during the first lunar night and rose to a maximum of 133° F during the second lunar day. Preliminary examination of the instrument photographs suggests that these temperature variations may be a result of unevenness in the thermal shroud. The shroud skirt appears to be raised off the surface at several places to the extent that significant reduction in the effective insulation might occur.

As recorded at the Apollo 12 and Apollo 14 sites, episodes of seismic disturbances are observed on the LP seismometers throughout the lunar day. These disturbances are most intense near times of terminator passage and are believed to be caused by thermal contraction and expansion of the Mylar thermal shroud that blankets the sensor.

FIGURE 8-2.–Seismometer after deployment on the lunar surface (AS15-86-11590).

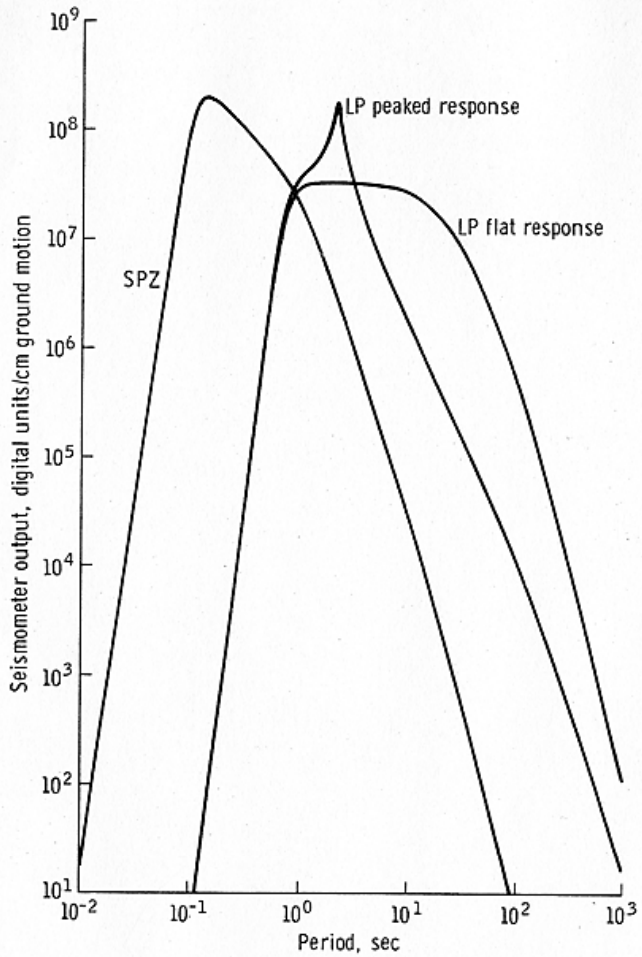

FIGURE 8-3.–Response curves for the LP and SP vertical-component seismometers. The ordinate scale is in digital units (DU) per centimeter ground motion amplitude. A DU is the signal variation that corresponds to a change in the least significant bit of the 10-bit data word.

RESULTS

The Apollo 15 PSE is a continuation of observations made during the Apollo 11, 12, 13, and 14 missions (refs. 8-1 to 8-8).

Preascent and Ascent Period

Before the LM ascent, many signals corresponding to various astronaut activities within the LM and on the surface were recorded, primarily on the SP vertical-component (SPZ) seismometer. Signals generated by the astronauts' footfalls and the motions of the Rover were detected at all points along the traverse (maximum range, approximately 5 km). A signal of particular interest during this period was generated by the thrust of the LM ascent engine. The signal began 0.69 sec after the burn began and lasted approximately 4.5 min. As shown in figure 8-4, a second arrival can be recognized that occurs 0.51 sec after the first arrival. By comparison with Apollo 14 active-seismic-experiment data and previous LM ascent signals, the first arrival is interpreted as a wave refracted along an interface with higher velocity material at depth. The second arrival has an apparent velocity of 92 m/sec and is interpreted as a wave traveling through the top (regolith) layer. This value is remarkably close to the regolith velocities of 104 and 108 m/sec measured at the Apollo 12 and Apollo 14 sites, respectively. The uniformity of results from widely separated sites indicates that the process of comminution by meteoroid impacts has produced a layer of remarkably uniform mechanical properties over the entire surface of the Moon. If a regolith depth of 5 m is assumed at the Apollo 15 site, the velocity of seismic waves in the underlying material is 185 m/sec.

Signals generated by movements of the Rover were detected by the SPZ seismometer to ranges of approximately 4 to 5 km. The maximum range of detection was limited during extravehicular activity by the large seismic-background level originating within the LM. The maximum range of detection would be approximately 10 km under normal quiescent conditions.

Starting and stopping of the Rover produced only gradual buildup and decay of the seismic-signal amplitude rather than abrupt changes in signal amplitude. This gradual change in amplitude can be explained as resulting from intensive scattering of seismic waves in the upper layer of lunar material. Measurement of the amplitude of the signal as a function of range for various frequency components will provide an estimate of the statistical distribution of scatterers in this surface zone. This analysis has not yet been completed.

Signals From Impacts of the SIVB and LM Ascent Stages

Signals from two manmade impacts (the SIVB stage and the LM ascent stage) were recorded as part of the Apollo 15 mission. The SIVB impact preceded emplacement of the Apollo lunar surface experiments package (ALSEP) used on the Apollo 15 mission and was recorded at both the Apollo 12 and the Apollo

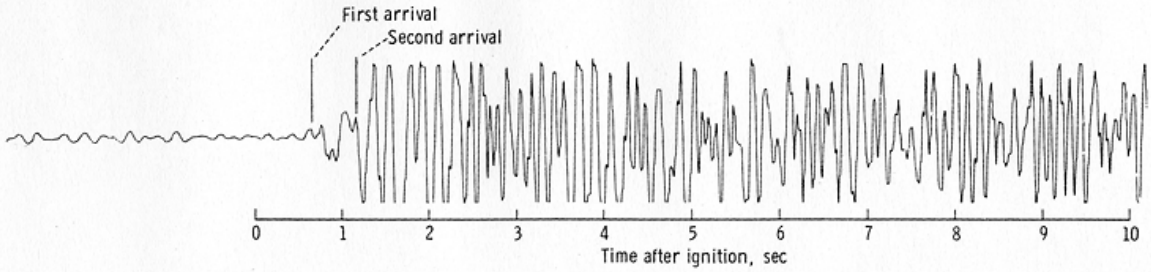

FIGURE 8-4.–Signal recorded by the SPZ seismometer from the lift-off of the Apollo 15 LM ascent stage.

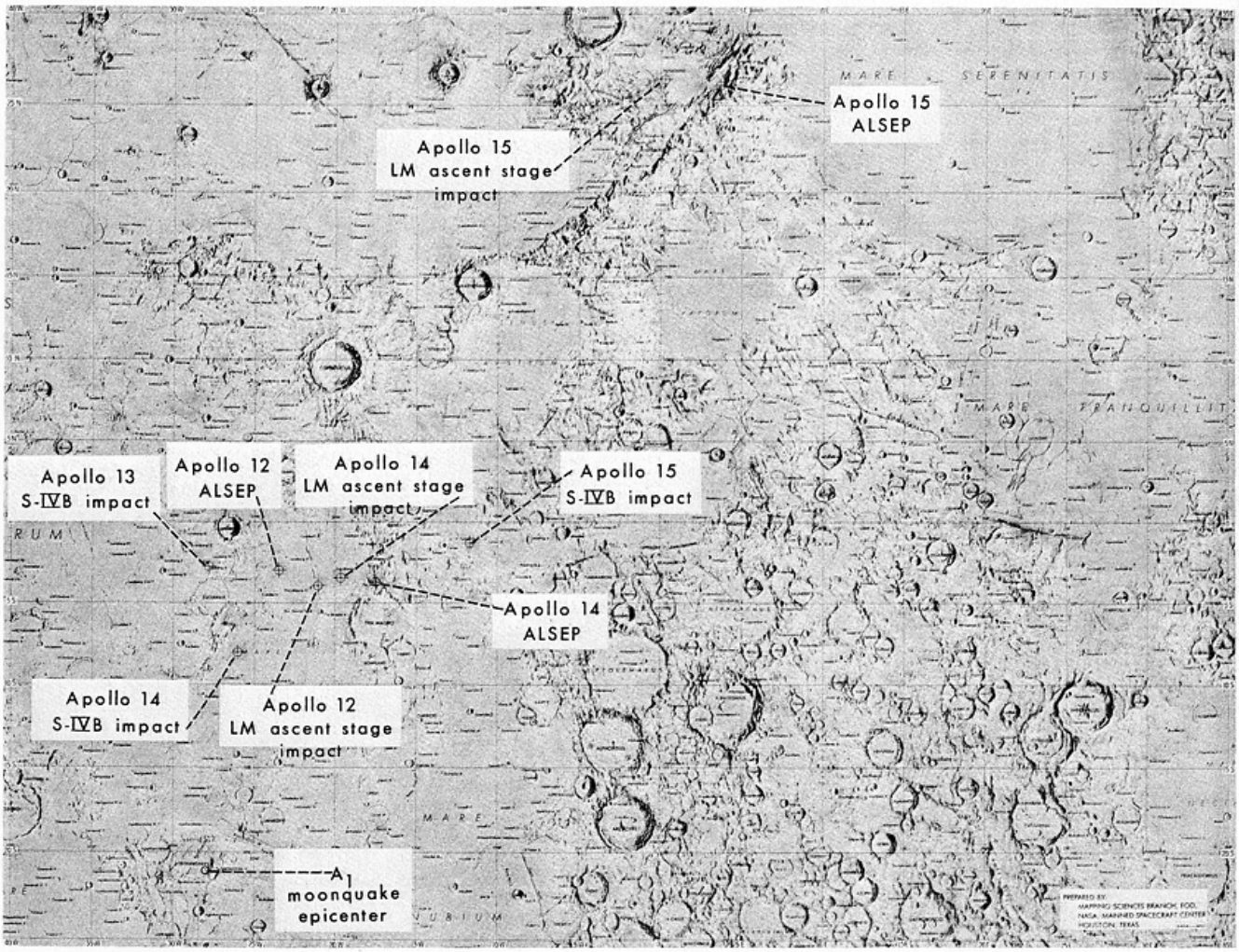

FIGURE 8-5.–Locations of ALSEP stations, LM, and SIVB impacts, and the epicenter of the most active source of moonquakes (A_1 zone).

14 stations, while the LM ascent-stage impact was also recorded at the Apollo 15 station. These impacts have aided greatly in understanding the lunar structure to a depth of approximately 80 km.

The locations of the three operating stations and all artificial impacts to date are listed in table 8-I and are also shown on the lunar map in figure 8-5. Relevant distances between these locations are also

TABLE 8-I.—*Coordinates of Seismic Stations, Impact Points, and Relevant Distances*

Location	*Coordinates*	*Distance, km, from —*		
		Apollo 12 site	*Apollo 14 site*	*Apollo 15 site*
Apollo 12 site	3.04° S, 23.42° W	—	—	—
Apollo 14 site	3.65° S, 17.48° W	181	—	—
Apollo 15 site	26.08° N, 3.66° E	1188	1095	—
Apollo 12 LM impact point	3.94° S, 21.20° W	73	—	—
Apollo 13 SIVB impact point	2.75° S, 27.86° W	135	—	—
Apollo 14 SIVB impact point	8.00° S, 26.06° W	170	—	—
Apollo 14 LM impact point	3.42° S, 19.67° W	114	67	—
Apollo 15 SIVB impact point	1.51° S, 11.81° W	355	184	—
Apollo 15 LM impact point	26.36° N, 0.25° E	1130	1049	93

listed in table 8-I. Pertinent parameters for the two impacts of the Apollo 15 mission are given in table 8-II.

The seismic signals from the last two artificial impacts, in compressed time scales, are shown in figure 8-6. These new impact signals are similar in character to previous impact signals. The signals are extremely prolonged, with very gradual increase and decrease in signal intensity and with little correlation between any two components of ground motion except at the first motion of the SIVB signal. Various distinctive pulses can be seen in the early parts of the records, but the only seismic phase that is identifiable with certainty is the initial P-wave arrival. These characteristics are believed to result from intensive scattering of the seismic waves in a highly heterogeneous outer shell, combined with low dissipation in the regions of the impact points and the seismic stations.

The initial portions of the new impact signals are shown in figure 8-7 on expanded time scales. The arrivals of the first P-waves and a tentatively identified shear wave (S-wave) are indicated in figure 8-7. The S-wave arrival has been identified on low-pass-filtered records and is not conspicuous in the broadband recording shown in figure 8-7. Traveltimes of these phases, together with those of previous manmade impact signals, are listed in table 8-III and are shown in figure 8-8. Detailed interpretation of the traveltime curves and related data are given in the section entitled "Discussion."

Short-Period Events

Several thousand signals with a great variety of shapes and sizes were recorded on the SPZ seismometer during the first 45 days of operation of the Apollo 15 PSE. The general level of recorded activity gradually subsided through the first lunar night after the initial activation of the PSE and increased abruptly at sunrise. Most of the events are attributed to venting or circulation of fluids and thermoelastic "popping" within the LM descent stage. The PSE is located approximately 110 m from the nearest footpad of the LM. The level of such activity was even higher during the operation of the Apollo 11 PSE but lower during the initial operating period of the Apollo 14 PSE. These relationships are explained by the smaller separation between the LM and the PSE in the Apollo 11 deployment (16.8 m) and by the greater separation between the LM and the PSE in the Apollo 14 deployment (178 m). These results cannot be compared with data obtained from the Apollo 12 SPZ seismometer because of the failure of that seismometer.

TABLE 8-II.—*Parameters of Apollo 15 Manmade Impacts*

Impact parameters	*SIVB*	*LM*
Day, G.m.t.	July 29	August 3
Range time,[a] G.m.t., hr:min:sec	20:58:42.9	03:03:37.0
Real time, G.m.t., hr:min:sec	20:58:41.6	03:03:35.8
Velocity, km/sec	2.58	1.70
Mass, kg	13 852	2385
Kinetic energy, ergs	4.61×10^{17}	3.43×10^{16}
Angle from horizontal, deg	62	3.2
Heading, deg	97	284

[a]Range time is the time that the signal of the associated event was observed on Earth.

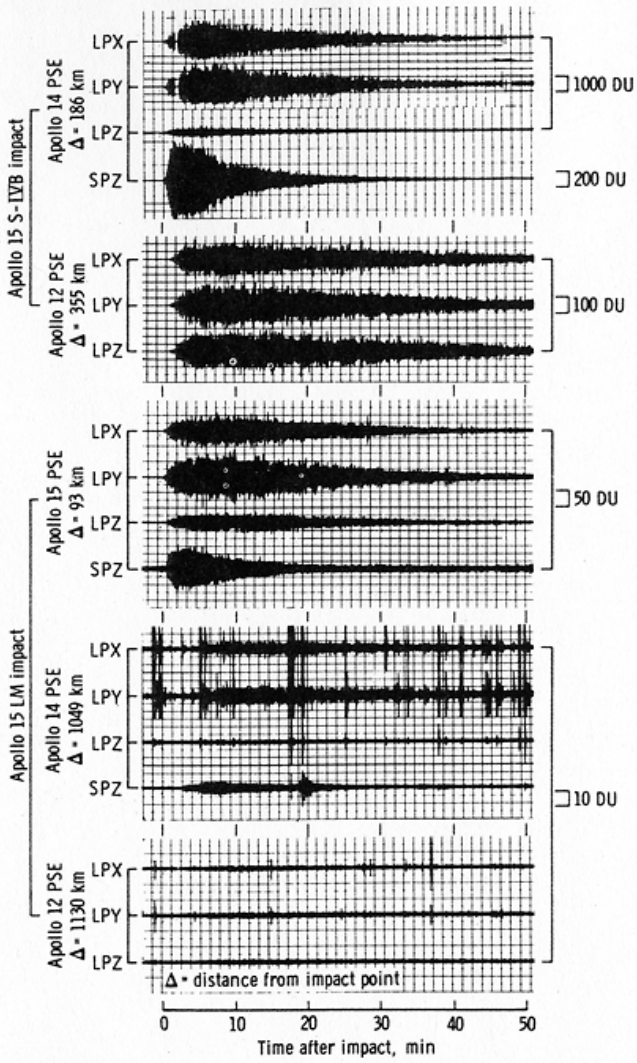

FIGURE 8-6.–Compressed time-scale records of the seismic signals received from the SIVB and LM impacts of the Apollo 15 mission at the Apollo 12, 14, and 15 ALSEP stations. The LPX, LPY, LPZ, and SPZ represent two long-period horizontal, long-period vertical, and short-period vertical components, respectively. For the amplitude scale DU, see figure 8-3.

The variation of SPZ seismometer activity is clearly related to the solar cycle at both the Apollo 14 and the Apollo 15 sites. The observed SPZ seismometer activity at the Apollo 14 site during the seventh and eighth lunations after deployment is shown in figure 8-9. Only SPZ seismometer events that show a gradual buildup and decay are included in figure 8-9. Events that have impulsive beginnings or very small rise times are probably generated by the LM or other equipment left on the Moon and are not included. Approximately 40 hours after sunrise at the Apollo 14 site, the number of observed SPZ seismometer events abruptly increases from a nighttime rate of four to five events per day to a daytime rate of between 30 and 50 events per day. This level of activity remains fairly constant until approximately 80 hours after sunset. At this time, the rate decreases abruptly to approximately 10 events per day, followed by a slower decrease to a nearly constant rate of four to five events per day approximately 5 days before sunrise. A similar pattern of activity is observed at the Apollo 15 site, but the level of activity is much higher than was detected during the first lunation at the Apollo 14 site, even though the LM and PSE separations at the two stations do not differ greatly. A rate of approximately 30 events per day was observed during the first lunar night after deployment of the Apollo 15 PSE as compared to a rate of four to five events per day for a nighttime period at the Apollo 14 site. This difference may indicate the presence of natural sources of seismic activity at the Apollo 15 site that are not present at the Apollo 14 site.

Possible sources of the observed SPZ seismometer activity at both the Apollo 14 and the Apollo 15 sites are thermal effects on the LM, the PSE thermal shroud, the cable connecting the sensor to the central station, other ALSEP instruments, the lunar soil, and nearby rocks. The phase lags noted between sunrise and the initiation of activity, and between sunset and the decrease in activity possibly reflect the thermal time constant of the source. Also, the continuing activity observed during the seventh lunar night at the Apollo 14 site suggests natural sources. Close meteoroid impacts and micromoonquakes would be possible sources for some of the signals. It is expected that more definite conclusions will be reached concerning the sources of signals recorded on the SPZ seismometers at the Apollo 14 and Apollo 15 sites, as the contribution from the LM descent stage at each station decreases during succeeding lunations. Then, the nighttime rate of SPZ seismometer activity common to both stations will set an upper limit on the possible meteoroid contribution, while a large discrepancy between the observed rates at the two stations would indicate a contribution from other sources near the more active station.

Natural Long-Period Events

Data on distant natural events come primarily from the LP seismometers. After an initial period of

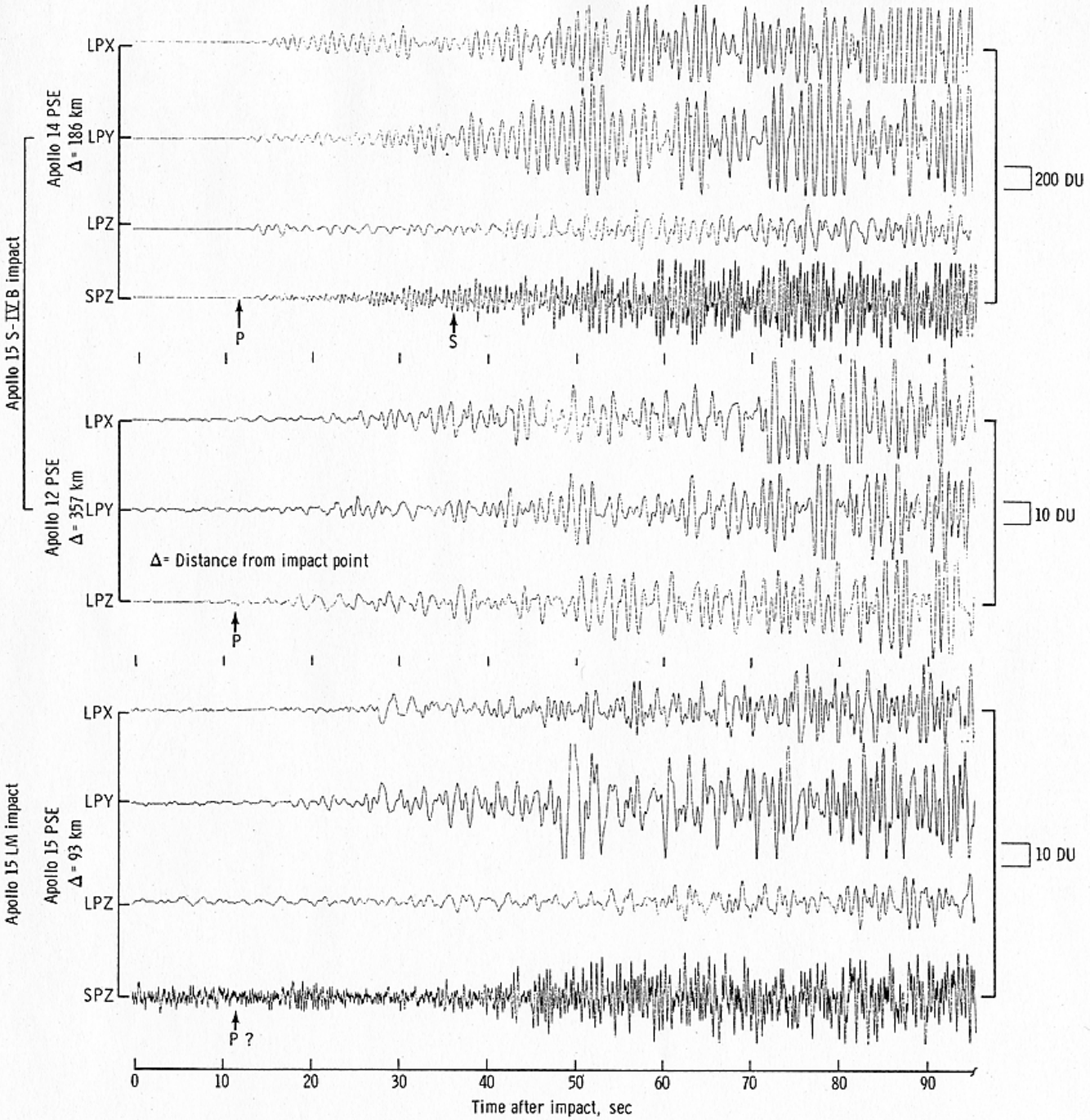

FIGURE 8-7.–Initial portions of the seismic signals from the Apollo 15 SIVB impact recorded at the Apollo 12 and Apollo 14 stations and from the Apollo 15 LM impact recorded at the Apollo 15 station. Zero on the time scale corresponds to 24.9 sec after impact for the top four traces, 44.1 sec after impact for the middle three traces, and 10.2 sec after impact for the bottom four traces. The earliest detectable signal is identified as the P-wave arrival, indicated by an arrow with the letter P. A later arrival, tentatively identified as the S-wave arrival from low-pass-filtered records and particle motion diagrams, is indicated by an arrow with the letter S.

TABLE 8-III.—*Observed Traveltimes of P-Wave and S-Wave Arrivals From LM and SIVB Impacts*

Impacting vehicle	*Station*	*Distance, km*	*P-wave traveltime, sec*	*S-wave traveltime, sec*[a]
Apollo 14 LM	14	67	17.8	31
Apollo 12 LM	12	73	ND[b]	NI[c]
Apollo 15 LM	15	93	[d]22?	NI
Apollo 14 LM	12	114	25?	45.0
Apollo 13 SIVB	12	135	28.6	50.5
Apollo 14 SIVB	12	170	35.7	55.7
Apollo 15 SIVB	14	186	36.6[e] (37.6)	60.5
Apollo 15 SIVB	12	357	55.5 (61)	NI
Apollo 15 LM	14	1049	ND	ND
Apollo 15 LM	12	1130	ND	ND

[a]All S-wave traveltimes are tentative because of uncertainties in identifying S-wave arrivals.
[b]ND = not detectable, signal amplitude below threshold of instrument detection capability.
[c]NI = not identifiable.
[d]Question marks indicate uncertain picks caused by noise background.
[e]Figures in parentheses indicate strong second arrivals.

days or weeks during which LM-generated high-frequency noise gradually subsides, these data can be supplemented by the SPZ seismometer data.

Seventy-five seismic signals were identified on the recordings from the Apollo 14 and Apollo 15 stations that were available from real-time data acquisition throughout the 42-day period after LM ascent. Continuous data from the Apollo 12 station were not available for this period because of limitations in the data decommutation capability at the NASA Manned Spacecraft Center (MSC). These data were retained on magnetic tape for future analysis. Based on signal characteristics, the detected events were classified either as moonquakes or impacts. Some of the signals were too small to be classified by the procedures used in this preliminary analysis. The results of this analysis are summarized in table 8-IV.

The criteria used for classifying seismic signals have been discussed in other reports (refs. 8-6 to 8-8), in which moonquakes and meteoroid impacts were identified as the sources of the recorded signals. Briefly, the signal characteristics that are useful in distinguishing a moonquake from a meteoroid impact are a short rise time and the presence of an H-phase. The H-phase of a moonquake is preceded only by low signal amplitudes and may be the first detectable motion of a weak event. The H-phase is a strong group of waves with a relatively sharp beginning, generally stronger on the horizontal components than on the vertical component, suggesting a shear-wave mechanism. The H-phase often contains lower frequencies than other portions of the record, peaking near the 0.5-Hz natural frequency of the LP seismometers. The maximum amplitude of the moonquake signal envelope is either at or only a few minutes after the H-phase.

Well-recorded signals also show an abruptly beginning, low-amplitude train that precedes and continues into the H-phase, suggesting a P-wave precursor. Numerous signals with these characteristics are found to fall into groups of matching signals (A_1 to A_{10}); members of each group have precisely identical waveforms. This property indicates a repeating moonquake focus to be the source of each group of matching signals. However, in this preliminary report, signal matching has been used in only a few cases to classify events because expanded time-scale playouts are required for the detailed phase comparisons.

In contrast with events containing an H-phase are numerous events (designated C-events) that have very emergent beginnings, smoothly varying envelope amplitudes, and no abrupt changes in signal frequency and amplitude. Because these are also the characteristics of artificial impact signals, C-events are believed to be meteoroid impacts. Unclassified events in table 8-IV are mainly those recorded too weakly to show diagnostic criteria on the drum seismograms.

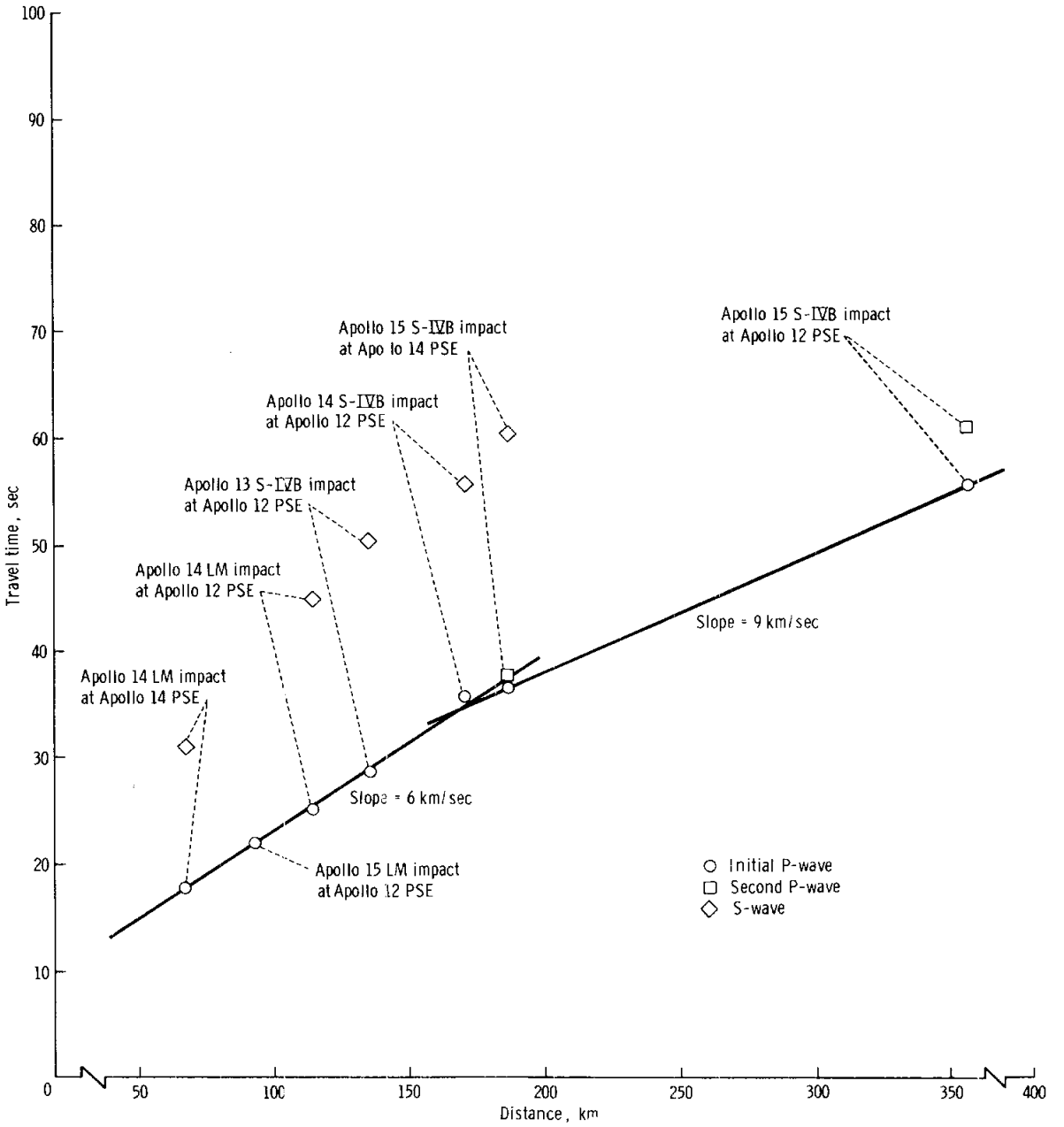

FIGURE 8-8.–Traveltimes of seismic waves recorded from the LM and SIVB impacts of the Apollo 12, 13, 14, and 15 missions. Circles indicate the first detectable arrivals, identified as P-wave arrivals. Squares are used to identify strong second arrivals. The S-wave arrival times are identified with much less certainty than the P-wave arrivals.

In table 8-IV, the number of moonquakes, impacts, and unclassified events during the 42-day period after LM ascent is given according to the stations at which the events were detected. Data in the three columns in table 8-IV are mutually exclusive; that is, an event counted at both the Apollo 14 and the Apollo 15 stations is not counted among those detected at only those stations. Fifty of the signals detected by the LP seismometers were also detected by the SP seismometer. These signals are

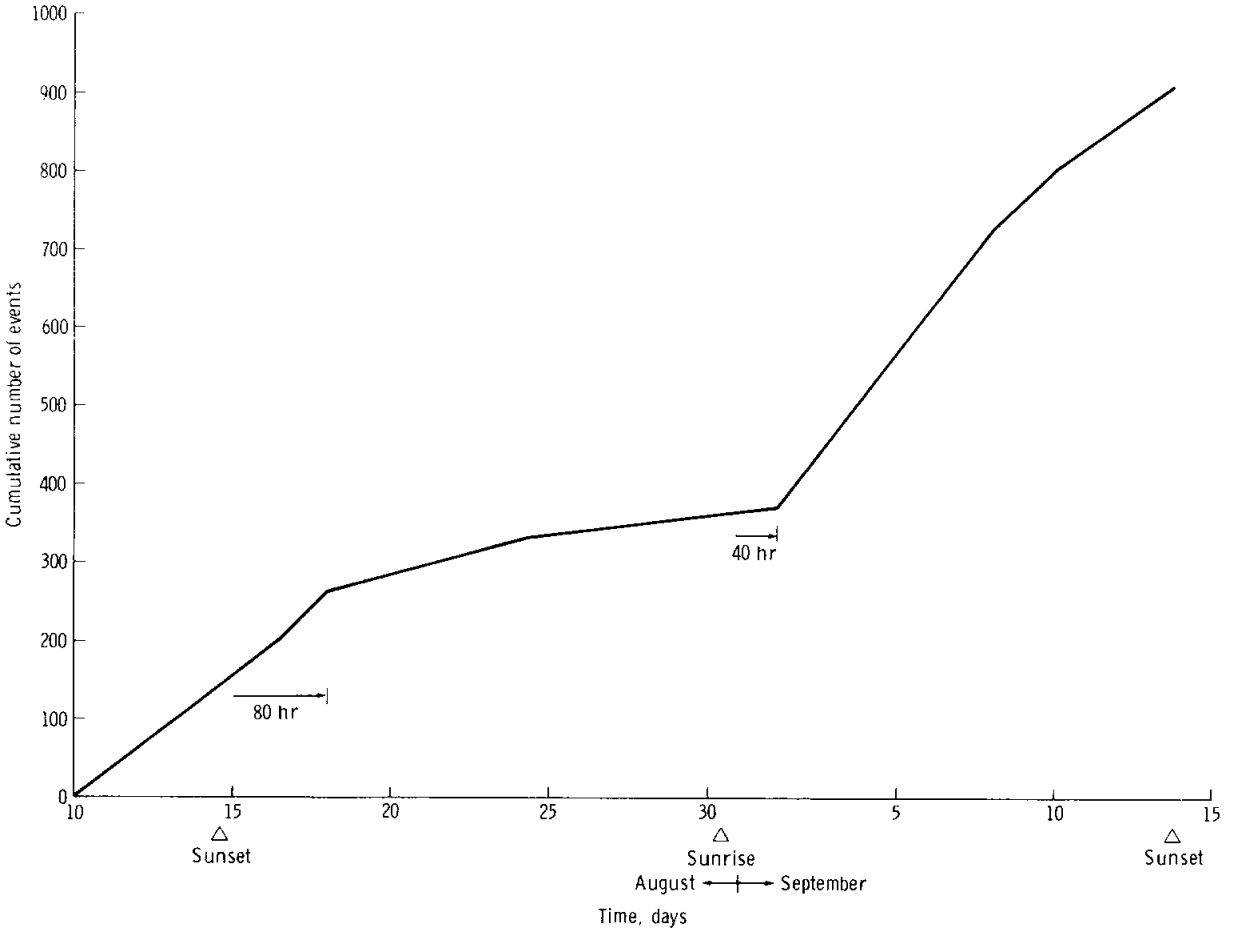

FIGURE 8-9.—Cumulative number of SPZ events observed at the Apollo 14 site as a function of time for the period August 10 to September 15. This time interval contains parts of the seventh and eighth lunations observed since deployment of the Apollo 14 PSE. Only SPZ signals that show a gradual buildup and decay are included. Signals that have impulsive beginnings or very short rise times are probably generated by the LM or other ALSEP instruments and are not included.

TABLE 8-IV.—*Seismic Events Recorded at Apollo 14 and 15 Sites*

Events	*Sites*			
	14	*15*	*14 and 15*	*Total*
LP event type				
Moonquake	11	0	11	22
Impact	26	4	5	35
Unclassified	16	1	1	18
Total LP	53	5	17	75
SP event type				
Moonquake	15	0	0	15
Impact	19	3	3	25
Unclassified	10	0	0	10
Total SP	44	3	3	50

counted in the lower part of table 8-IV. Signals detected by the SPZ seismometer only were not included in the listing. Classification of the SP events is based primarily on the character of the corresponding LP signals.

The cumulative distributions of the maximum amplitudes of the signal envelopes for the various categories of events are plotted in figure 8-10. The slope of such curves is a measure of the relative abundance of large and small events. The separate curves, which show the contributions of all events, all moonquakes, and all impacts for each station, are discussed in the following paragraphs.

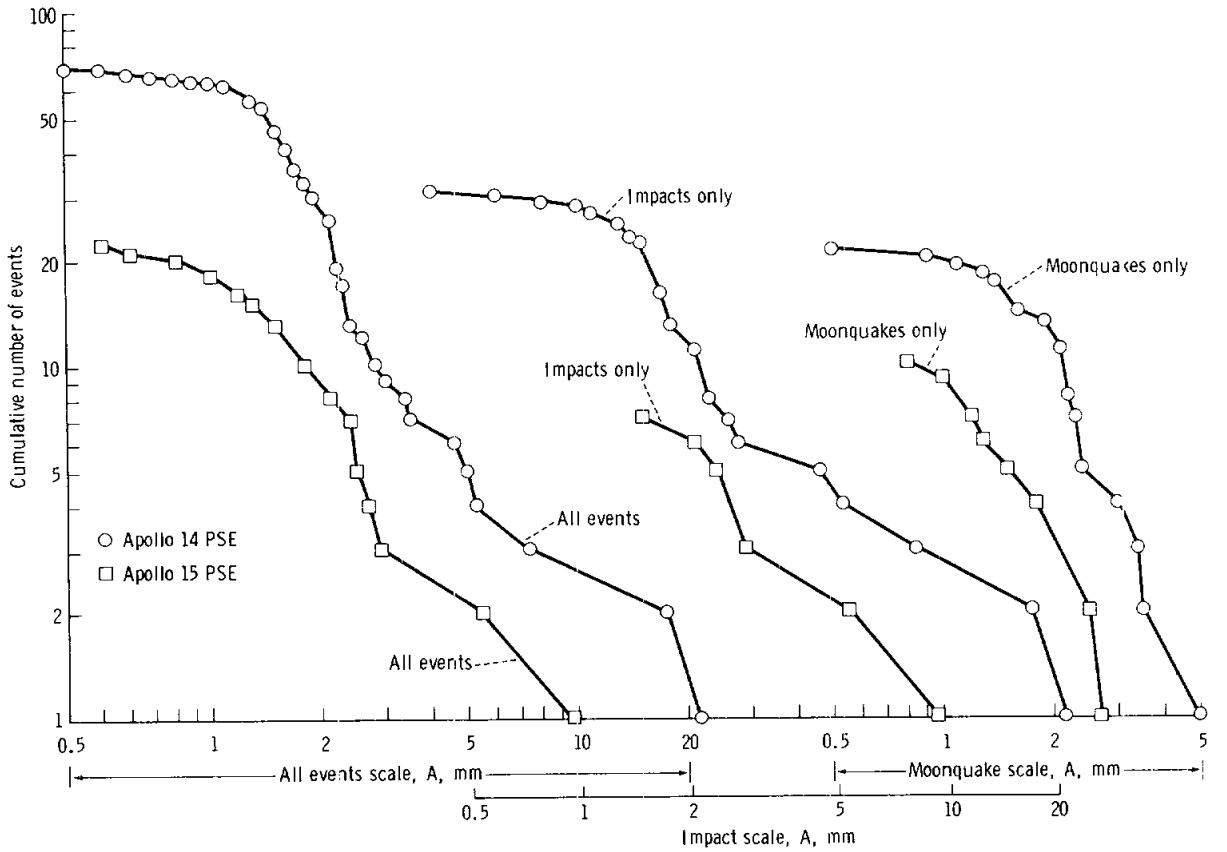

FIGURE 8-10.—Cumulative curves of LP amplitude data for natural events. Data used are amplitude measurements of the events represented in table 8-IV covering a 42-day period from LM lift-off August 2, 17:11 G.m.t., to September 13, 17:58 G.m.T. The amplitude variable $A = (X^2 + Y^2 + Z^2)^{1/2}$ where X, Y, and Z are the maximum peak-to-peak amplitudes of the smoothed envelopes of seismic signals recorded by the LP seismometers. Each plotted point (n,A) represents the number of events that have amplitude A or greater in the group represented by the particular curve. Unclassified events are included with the "all events" data but not with the impact or moonquake data.

A new data-processing technique that enhances very small signals has revealed that episodes of frequent small moonquakes occur. These episodes begin and end abruptly with no conspicuously large event in the series. By analogy with similar Earth phenomena, these signals are referred to as moonquake swarms. Examples of swarm activity are shown in the curve of figure 8-11. The slope of this curve is proportional to the rate of occurrence of moonquakes detected at the Apollo 14 station as a function of time from April 7 to May 10. Four intervals of increased activity occurred during this period. Two similar swarms occurred from May 16 to 20 and from May 25 to 29. Three swarms were detected at the Apollo 12 and Apollo 14 stations during the month after activation of the Apollo 15 station. Signals from moonquake swarms are not detectable by visual inspection of the real-time recordings from the Apollo 15 station for this period. However, additional data processing will be required to reach a definite conclusion on this point.

DISCUSSION

Scattering of Seismic Waves and Near-Surface Structure of the Moon

The characteristic long duration of lunar seismic

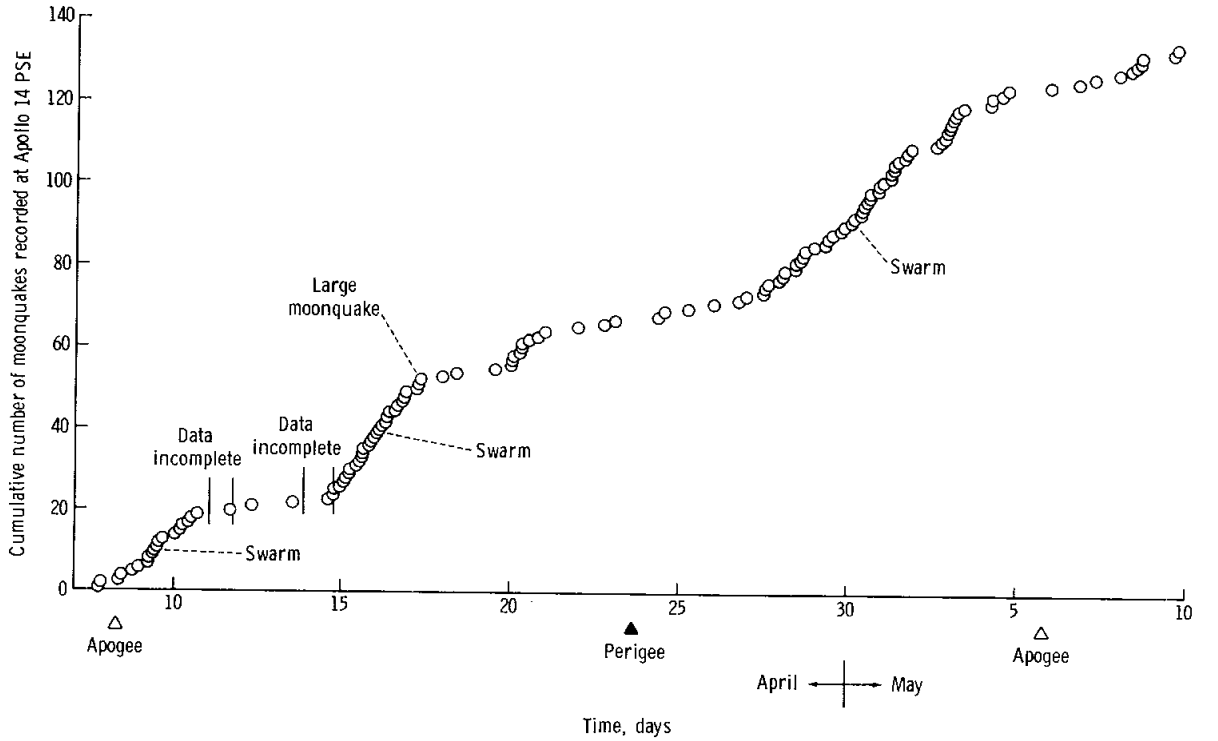

FIGURE 8-11.–Cumulative number of LP events observed at the Apollo 14 site as a function of time for the period April 7 to May 10. All LP events observed during this interval are included. Moonquake swarms appear as abrupt increases in the cumulative number of events. During periods of swarm activity, a rate of eight to 12 events per day is observed as compared to the normal rate of one to two events per day. Many of the swarm events are also detected at the Apollo 12 station.

wave trains has been interpreted as resulting from intensive scattering of seismic waves in a heterogeneous surface layer that probably blankets the entire Moon (refs. 8-1 to 8-7). Transmission of seismic energy below the scattering zone is believed to be highly efficient. This hypothesis is further confirmed by the data obtained during the Apollo 15 mission.

In figure 8-12, the rise times of artificial impact signals measured on narrowband-filtered seismograms are plotted against distance. The rise times increase with distance (and decreasing frequency) at near ranges, reach a maximum value at 100 to 150 km, and remain nearly at this level at greater distances. Seismic rays emerging at 100 to 150 km penetrate approximately 15 to 20 km into the Moon. Thus, the scattering zone must be of this thickness or less. However, a zone a few kilometers thick may account for the observed scattering. Below this level, the lunar material must behave more nearly as an ideal transmitter of seismic waves to produce no further significant increase in rise time at far distances.

In such a lunar structure, seismic waves generated by an impact are intensively scattered near the source and are observed as a scattered wave train in the near ranges. A part of this energy leaks into the lunar interior as a prolonged wave train, propagates through the lunar interior without significant scattering, undergoes further scattering when it returns to the surface, and is observed as a prolonged wave train at a distant seismic station. Therefore, the degree of scattering does not depend on the distance at far ranges. The relatively short rise times of moonquake signals are explained by the fact that seismic energy from a deep source must propagate through the scattering zone only one time en route to a seismic station.

The rise-time variation in the far ranges is irregular. This irregularity may reflect geographic differences in

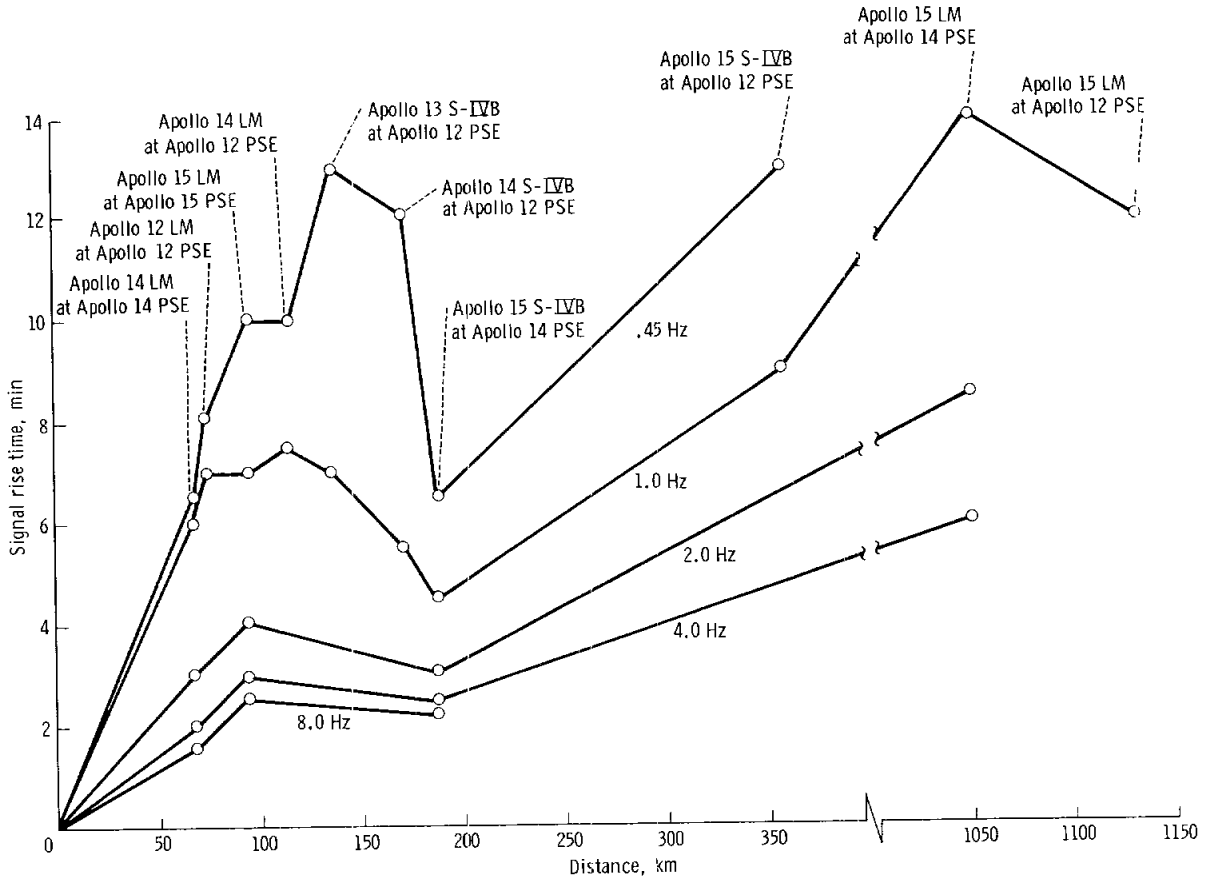

FIGURE 8-12.—Rise times of LM- and SIVB-impact signals measured on narrowband-filtered LPZ and SPZ seismograms. Four-pole Butterworth filters were used to produce the filtered seismograms. The rise time is measured from the time of impact to the approximate peak of the signal strength. The apparent trough in the rise-time curve at approximately 180 km coincides with the focusing of seismic energy at this range evidenced by enhancement of the P-wave amplitudes and the amplitudes of signal envelope maximums.

the complexity of the scattering zone. Important details of the scattering zone have not yet been determined; however, it is evident that abundant craters of various sizes and associated structural disturbances near the surface of the Moon must be elements of this unusual structure. Further study of the rise-time data of a large number of lunar events will eventually lead to a more quantitative description of the lunar scattering zone.

Lunar Structure Below the Scattering Zone

Information about the lunar structure can be obtained from the traveltimes, amplitudes, and angles of emergence of P-waves. The traveltimes provide the most directly interpretable data, whereas the other information supplements these data for determining the finer features of the velocity profile.

As shown in figure 8-8, the observed traveltime curve between distances of 67 and 186 km can be represented by a nearly constant apparent velocity of 6 km/sec. Deviations from a straight line in this range are less than 1 sec, despite the fact that these data represent traveltimes over paths with widely varying azimuths. This observation indicates that the outer 25 km of the Moon is fairly uniform in various directions in the region of the Apollo 12 and Apollo 14 stations.

The nearly constant apparent velocity of 6 km/sec in this distance range means that the P-wave velocity is nearly constant at 6 km/sec in a certain depth range

in the lunar interior. How the P-wave velocity increases from approximately 300 m/sec at a depth of less than 76 m, as observed by the active seismic experiment (ASE) at the Apollo 14 site (ref. 8-9), to 6 km/sec is uncertain because of the gap in traveltime data between ranges of a few hundred meters (ASE range) and 67 km (Apollo 14 LM impact). However, it can be deduced from these data that the P-wave velocity must equal or exceed 6 km/sec at a depth of 15 to 20 km; 6 km/sec is close to values measured in the laboratory on lunar igneous rock under high pressure (refs. 8-10 and 8-11). Thus, the assumption can be made that the seismic wave velocity to depths of approximately 20 to 25 km is about the same as the velocity found at corresponding confining pressures in the laboratory. Traveltimes predicted from such a model of the lunar interior, adjusted to match the near-surface ASE findings, are found to be in close agreement with the observed traveltimes to a distance of 170 km. Thus, the simplest model consistent with the data would consist of loosely consolidated material in the near-surface zone, self-compacted to yield a strong increase in velocity with depth, with a gradual transition to more competent rock below. The velocity increases as a result of pressure and reaches 6 km/sec at a depth of between 15 and 20 km. The effects of compaction by meteoroid impacts, which may be important in the upper few kilometers, have been ignored.

An important new finding of the Apollo 15 mission is that an apparent velocity of 9 km/sec is observed between distances of 186 and 357 km as determined from recordings of the Apollo 15 SIVB impact at the Apollo 14 and Apollo 12 stations, respectively. Explanations of this high apparent velocity in terms of lateral inhomogeneities and local structural effects in material with a velocity of 6 km/sec or less appear to be unsatisfactory. Thus, it is concluded that a layer with a P-wave velocity of approximately 9 km/sec exists below a depth of 25 km in the lunar interior. Whether the transition from 6 to 9 km/sec is gradual or sharp cannot be determined from the available traveltimes alone.

More detailed information on lunar structure can be obtained when other associated data, such as signal-amplitude variations and second arrivals, are also taken into account. The observed variation of the maximum P-wave amplitudes for the LM and SIVB impact signals is shown in figure 8-13. From this plot, it can be seen that the LM data must be adjusted upward by a factor of 17.4 to yield values that fit smoothly on the curve for the SIVB data. This factor is required to compensate for the lower kinetic energy and much shallower angle of the LM impact. Except for the two data points near 180 km, the P-wave amplitude decreases monotonically in approximate proportion to the -1.5 power of the distance. The P-wave amplitudes at 170 and 186 km are greater than the base-level amplitude by a factor

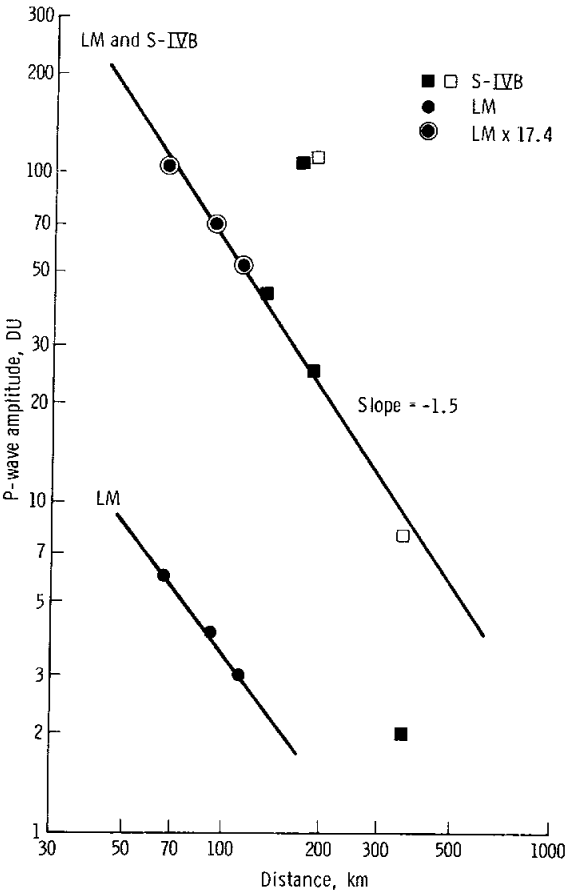

FIGURE 8-13.–Maximum peak-to-peak amplitudes, in digital units, of P-wave arrivals from the LM and SIVB impacts of the Apollo 12, 13, 14, and 15 missions, recorded by the LP seismometers. Each LM had nearly the same kinetic energy of approximately 3.3×10^{16} ergs at impact; each SIVB had nearly the same kinetic energy of approximately 4.6×10^{17} ergs at impact. The LM signal amplitudes are adjusted upward by a factor of 17.4 to give a smooth fit to the SIVB data. This empirically determined factor is required to compensate for the lower kinetic energy and shallower angle of the LM impacts relative to the SIVB impacts. The digital unit is defined in figure 8-3.

of 4.5, corresponding to an energy concentration of a factor of 20. This observation indicates that the lunar structure is such that focusing of seismic energy occurs in this range interval. A change in the slope of the travel-time curve, from 6 km/sec to a higher velocity, also occurs in this range interval. Both amplitude and travel-time variations require that the P-wave velocity begin to increase at a depth of between 20 and 25 km, to higher velocities below. Thus, a change in composition or phase at a depth of between 20 and 25 km is inferred.

Strong secondary arrivals from the Apollo 15 SIVB impact, as plotted in figure 8-8, can be interpreted as resulting from the presence of an intermediate layer with a P-wave velocity approaching 7.5 km/sec and a thickness of between 30 and 50 km. Arrivals after the initial P-wave must be treated with caution, however, because of the possibility that they may correspond to multipaths through an irregular medium. This ambiguity can be resolved only by obtaining additional impact data in this region, as is presently planned for the Apollo 16 mission.

Additional data to aid in the determination of detailed lunar structure are horizontal-to-vertical amplitude ratios of P-wave arrivals (fig. 8-14). The horizontal-to-vertical amplitude ratio is a direct measure of the P-wave incident angle and thus is an indication of the relative velocity at the deepest point where each seismic ray penetrates. This ratio decreases with increasing distance, indicating a gradual increase of velocity from the penetration depth of the ray emerging at 67 km (approximately 13 km) to the penetration depth of the ray emerging at 186 km (approximately 25 km). A quantitative interpretation of the data requires a knowledge of the velocity structure within the upper few kilometers of the lunar interior. Conversely, because the velocities at depth are known from the traveltime curve, the velocity structure in the upper few kilometers of the lunar interior can be deduced from the horizontal-to-vertical amplitude ratio. This latter step has not yet been completed.

Two interpretations of the P-wave arrival data representing the range of likely models for the upper 80 km of the lunar interior are shown in figure 8-15. In model 1, the transition in P-wave velocity from 6 to 9 km/sec is gradual; model 2 introduces two abrupt changes. In both models, the thickness of the surface crustal layer is between 20 and 25 km. The P-wave velocity reaches approximately 6 km at the

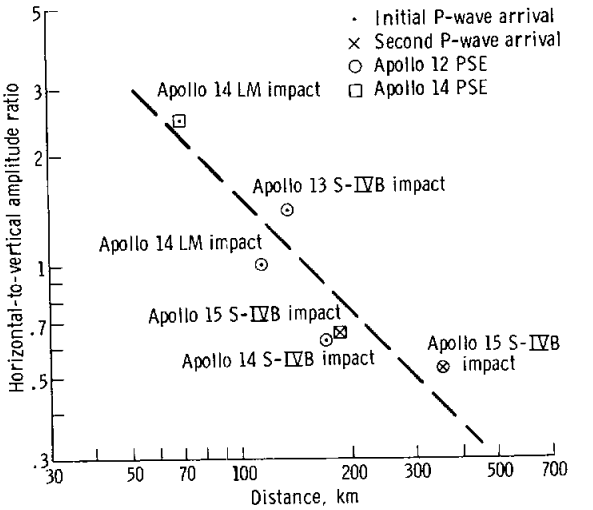

FIGURE 8-14.–Horizontal-to-vertical amplitude ratios of major P-wave arrivals from LM and SIVB impacts of the Apollo 12, 13, 14, and 15 missions, as recorded by the LP seismometers. The ratio is greater than 1 when the ground-particle motion is more nearly horizontal than vertical. Aside from the use of this diagram in interpreting velocity structure in the lunar interior, the range dependence seen in this diagram may also be used for estimating distances to large meteoroid impacts in this distance range.

base of this layer. The top zone of the layer (the scattering zone) is a zone in which the velocity increases rapidly with depth as a result of self-compaction and in which seismic waves are intensively scattered. The velocity below layer 1 may increase gradually, reaching 9 km/sec at a depth of between 60 and 70 km (model 1); or it may reach a constant velocity of 7.5 km/sec, with a sharp transition to 9 km/sec at a depth of between 55 and 70 km (model 2). Thus, the zone below the top layer may be a transition zone or it may be a second crustal layer with a thickness of between 30 and 50 km and a P-wave velocity of 7.5 km/sec, overlying the higher velocity mantle. The presence of deeper discontinuities is not precluded by present data.

The identification of shear waves in the impact signals is sufficiently uncertain that discussion of structural interpretation based upon their traveltimes must be deferred until further analysis can be completed. Similarly, it is expected that further study of body-wave arrivals from moonquakes and meteoroid impacts will aid in further elucidation of lunar structure.

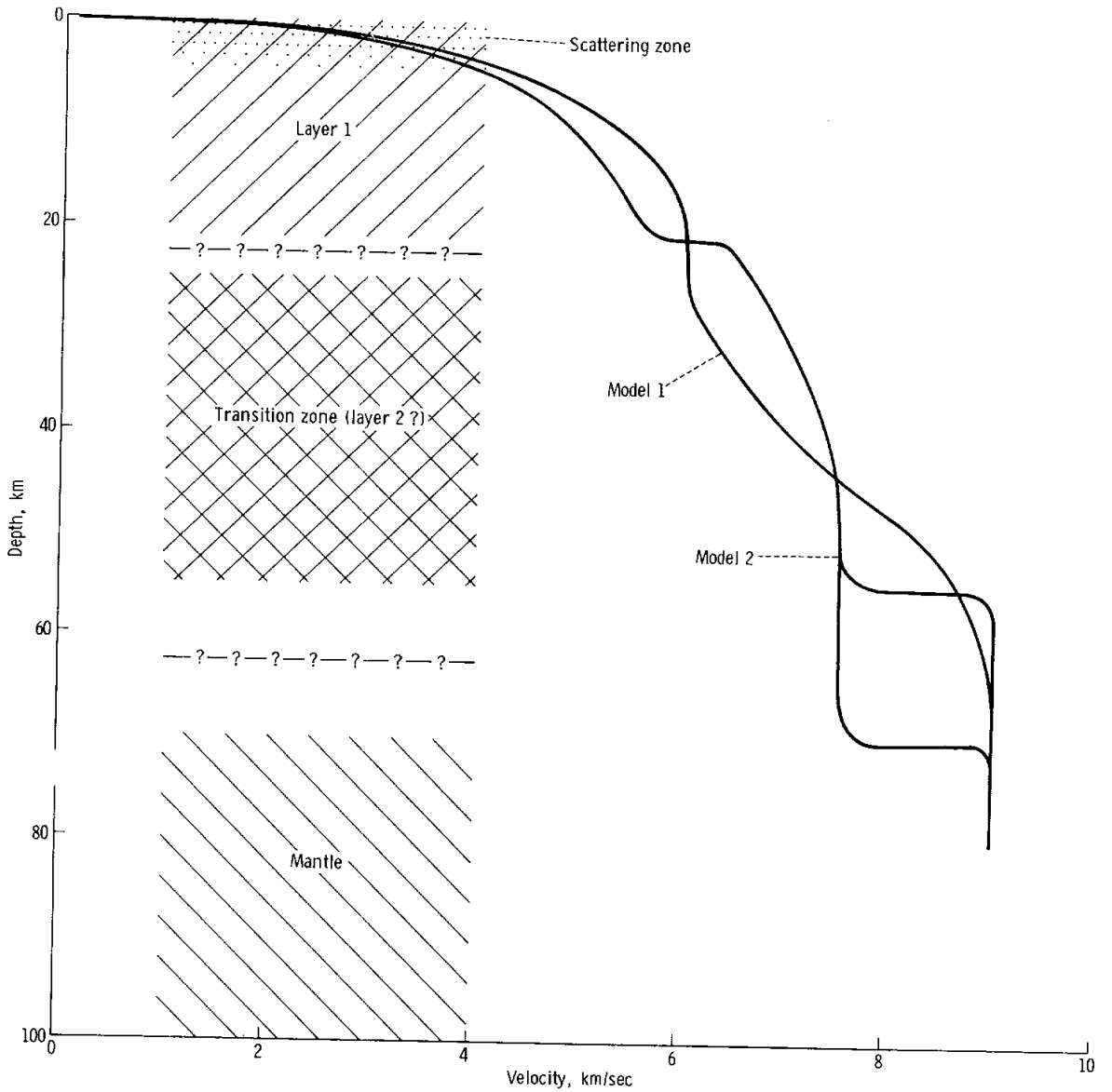

FIGURE 8-15.—A tentative P-wave velocity profile in the upper 80 km of the lunar interior deduced from P-wave arrivals from the LM and SIVB impacts of the Apollo 12, 13, 14, and 15 missions.

No P-wave traveltime data are available at present beyond a distance of 357 km corresponding to a depth of penetration of approximately 80 km. However, other features of the signal wave train, such as the peak-to-peak amplitude of the signal envelope and the rise time of the signal, can be used to interpret the structure of the lunar interior below this depth.

The maximum peak-to-peak amplitude of the signal envelope shows an almost monotonic decrease with increasing range in figure 8-16 for both the SIVB and the LM-impact data. The only exception is the amplitude generated by the Apollo 15 SIVB at the Apollo 14 station (range, 186 km), which is somewhat larger than the amplitude of the Apollo 14 SIVB impact recorded at the Apollo 12 station

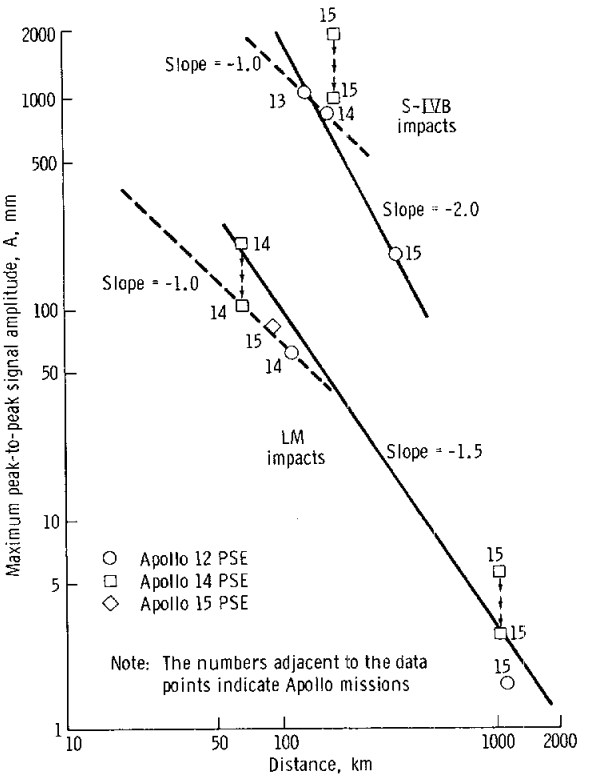

FIGURE 8-16.—Peak signal amplitudes A as a function of ranges r of artificial-impact recordings. The amplitude given is $A = (X^2 + Y^2 + Z^2)^{1/2}$, where X, Y, and Z are the maximum peak-to-peak amplitudes (mm) of unfiltered signal envelopes recorded at full gain on the three LP component seismograms. Data of the Apollo 13, 14, and 15 SIVB impacts and of the Apollo 14 and 15 LM impacts are shown. The SIVB-impact data form an upper group of points, and LM-impact data fall in a lower group. The Apollo 14 station amplitudes are plotted at their observed values and also as reduced by a factor of 2.0 to correspond to the observed average difference in sensitivity between the Apollo 12 and Apollo 14 stations. The slopes of lines drawn through various sets of data indicate a range variation of amplitude between $r^{-1.0}$ and $r^{-2.0}$

(range, 170 km), even after allowing for the higher sensitivity of the Apollo 14 station. This difference is probably a result of the focusing effect at this range. Also, as for P-wave amplitudes, the maximum signal-envelope amplitudes for SIVB impacts cannot be compared directly with those of LM impacts for two reasons: the shallow impact angle of LM vehicles (3.3° to 3.7° from the horizontal) introduces uncertainty as to the seismic coupling efficiencies of LM impacts; also, the coupling efficiency of an SIVB impact may greatly exceed that of an impact of the LM ascent stage because the greater kinetic energy causes penetration into harder material. At ranges of as much as 170 km, an amplitude variation as $r^{-1.0}$ is satisfactory for LM and SIVB data, separately. The amplitude of the Apollo 15 LM impact at the Apollo 15 station also fits this variation. Stronger falloff, at least for distances beyond 186 km, is indicated by the Apollo 15 longer range data.

In figure 8-17, all SIVB-generated amplitudes that are shown in figure 8-16 have been divided by a factor of 20. This conversion factor provides a smooth overlap between the LM and SIVB amplitude data. The data can be fit by two straight-line segments intersecting at approximately 200 km. The simple, near-range variation as r^{-1} was noted in reference 8-7. It is apparent that a distance variation of approximately $r^{-1.8}$ is required at greater ranges. The range dependence of $r^{-1.8}$ and the LM/SIVB adjustment factor of 20 determined for the maximums in the signal envelopes both agree reasonably well with the values of $r^{-1.5}$ and 17.4 found independently from the P-wave amplitudes.

The Absence of Surface Waves and Surface-Reflected Phases

The major differences between terrestrial and lunar seismic signals now appear to be explained by the presence of a heterogeneous surface layer that blankets the Moon to a probable depth of several kilometers, with a maximum thickness of 20 km. Seismic waves with the observed wavelengths are intensively scattered within this zone. Seismic wave velocities and absorption of seismic energy are both quite low in this zone. The acoustic properties of this zone, the scattering zone, can probably be explained as the result of meteoroid impacts and the nearly complete absence of fluids. The lower boundary of the scattering zone is the depth below which the rock, conditioned by pressure, transmits seismic waves without significant scattering.

The presence of the scattering zone probably accounts for two features of lunar seismic signals that earlier puzzled the experiment team: (1) the absence of normal surface waves (Love waves and Rayleigh waves) and (2) the poor definition or total absence of identifiable surface-reflected phases, particularly from deep moonquakes.

Surface waves, with wavelengths of approximately the thickness of the scattering zone and smaller, will

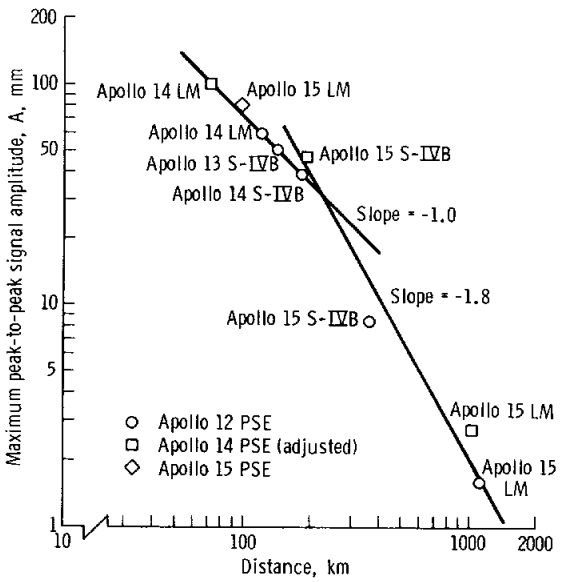

FIGURE 8-17.–Adjusted variation of artificial-impact amplitude with range. The data points of figure 8-16 are replotted with the same abscissas. Ordinates of SIVB amplitude data are plotted after division by a factor of 20. All Apollo 14 station data are adjusted for relative station sensitivity by dividing amplitude values by 2.0. With these adjustments, an amplitude variation as $r^{-1.0}$ for ranges 67 to approximately 200 km and as $r^{-1.8}$ at greater ranges is a satisfactory representation of the available data.

scatter quickly into body waves within the scattering zone and thus will propagate only to very short ranges. Surface waves long enough to propagate coherently (signal periods greater than approximately 5 sec) would be generated only by events larger than any that have occurred during 20 months of observation. Such events must be rare.

A thin surface zone of intensive scattering, coupled with a rapid increase of seismic velocity with depth, will make the lunar surface a very poor reflector for seismic waves incident on the surface from the lunar interior. In such a structure, a small proportion of the incident seismic energy follows the simple ray path of total reflection. Most of the energy is trapped in the surface region and leaks out slowly as from a primary surface source. As a result, no sharp increase of seismic energy is observed at a time when a surface-reflected seismic phase is expected from an event at a large distance. Phases corresponding to surface-reflected P- and S-waves have been tentatively identified in several of the LM and SIVB signals, but they are poorly defined.

Location and Focal Mechanism of Moonquakes

Moonquakes detected at the Apollo 12 and Apollo 14 stations before the Apollo 15 mission are believed to have originated at no less than 10 different focuses, although some of these may be quite close to one another. However, a single focus (A_1 zone) accounts for nearly 80 percent of the total detected seismic energy. Two moonquakes from the A_1 zone were recorded by the three stations of the Apollo seismic network during the first two perigee periods after activation of the Apollo 15 station, with one moonquake at each perigee. Both moonquakes were small to intermediate in size relative to the range of A_1 signal amplitudes detected thus far. The P-waves from these events arrived at the Apollo 12 station 1.8 sec earlier than at the Apollo 14 station but could not be detected at the Apollo 15 station. Shear waves (H-phase) arrived first at the Apollo 12 station, and 3.4 sec and 113.9 sec later at the Apollo 14 and Apollo 15 stations, respectively. Using these arrival times and the lunar models shown in figure 8-15, the epicenter (point on the surface directly above the moonquake focus) is located at latitude 21° S and longitude 28° W, approximately 600 km south-southwest of the Apollo 12 station, as shown in figure 8-5. The depth of the focus is approximately 800 km, somewhat deeper than any known earthquake. The remaining moonquake focuses have not yet been located.

The source of strain energy released as moonquakes is not known; but, if significant depth of focus for all moonquakes is verified by future data, these data will have profound implications concerning the lunar interior. In general, this result would require that, unlike the Earth, the shear strength of the lunar material at a depth of 800 km must be large enough to sustain appreciable stress and that maximum stress differences originate at this depth. These conditions place strong constraints on the temperature distribution in the deep lunar interior.

The nearly exact repetition of moonquake signals from a given focal zone over periods of many months requires that the focal zones be small, 10 km in diameter or less, and fixed in location over periods approaching 2 yr. If moonquake focuses were

separated by as much as 1 wavelength, larger differences would be observed among moonquake signals.

As noted previously (refs. 8-5 to 8-8), the moonquakes occur in monthly cycles near times of apogee and perigee. This phenomenon suggests that the moonquakes are triggered by lunar tides. This hypothesis is strengthened by the observation that the total seismic-energy release and the interval between the times of occurrence of the first moonquakes each month and times of perigee both show 7-month periodicities which also appear in the long-term gravity variations. With a few possible exceptions, the polarities of signals belonging to a set of matching events are identical. This observation implies that the source mechanism is a progressive dislocation and not one that periodically reverses in direction. Conceivably, detectable movements in one direction may be compensated by many small, undetectable movements in the opposite direction. A progressive source mechanism suggests a secular accumulation of strain periodically triggered by lunar tides. Whether this strain is local, regional, or moon-wide is an intriguing problem for further study. Several possible sources are slight expansion of the Moon by internal radiogenic heating or slight contraction on cooling, a gradual settling of the lunar body from an ellipsoidal form to a more nearly spherical form as the Moon gradually recedes from the Earth, localized strains caused by uncompensated masses, or localized thermal stresses.

For samples of earthquake data, the cumulative amplitude curves often have a nearly linear slope known as the b-value. The b-values measured for tectonic earthquakes are normally close to 1. The b-values of moonquake data in figure 8-10 are approximately 2. Higher b-values, as measured for moonquakes, are typical of one class of earthquakes —those associated with volcanic activity, which are presumably generated by subsurface movements of magma.

Laboratory experiments have demonstrated that high b-values are associated with microfracturing in rock samples subjected to small mechanical stresses (ref. 8-12) and with cracking from thermal stresses induced by heating and cooling of samples (ref. 8-13). High b-values are also measured in laboratory tests when two surfaces are rubbed together under high pressure (ref. 8-14). Thus, although no definite conclusion regarding the focal mechanism of moonquakes can be based on b-value data alone, comparison of laboratory experimental data and seismic measurements for earthquakes suggests that moonquakes may be generated by thermal stresses, possibly of volcanic origin; tectonic stresses at low stress levels; or dislocations along preexisting fractures. These are tentative suggestions, but they serve as hypotheses against which future data will be tested.

Moonquake Swarm Activity

To date, one of the most significant discoveries of lunar seismology is the observation of moonquake swarms. Each swarm is a distinctive sequence of moonquakes closely grouped in space and time, generally containing no conspicuous event. The lunar seismic activity detected between April 7 and May 10 by the Apollo 12 and Apollo 14 LP seismometers is shown in figure 8-11. Two major and two or three minor moonquake swarms occurred during this interval. Other swarms were observed between May 16 to 20 and between May 25 to 29. A moonquake swarm is characterized by an abrupt beginning and ending of activity. Events are recorded at a nearly constant rate of eight to 12 per day during the swarm, as compared to one or two per day between periods of swarm activity. Swarms, unlike other moonquake activity observed to date, do not appear to correlate with lunar tides.

Swarm events appear to be moonquakes because they have some of the characteristics of category A (matching) moonquakes, such as prominent H-phases, low-frequency spectra, and relatively small rise times. Also, the pattern of activity suggests that individual events of a particular swarm are not isolated or unrelated but that they represent an extended process occurring within a limited source region. However, swarm moonquakes differ from previously identified moonquakes. Unlike category A moonquakes, the swarm moonquakes do not appear to have matching waveforms. The waveforms of six of the largest swarm moonquakes do not match in detail among themselves nor with any other event, although the three largest moonquakes of the May 16 to 20 swarm show some similarities. The smaller swarm events have not yet been examined in detail. By contrast, no large differences in the category A_1 moonquake signals recorded at the Apollo 12 station have been observed during a period of 20 months. Thus, although the dimension of the category A_1 focal zone

is thought to be approximately 1 wavelength (10 km) or less, the nonmatching swarm events must be separated by at least 1 wavelength or more. A swarm of 30 moonquakes must be distributed throughout a minimum volume of approximately 10^4 km^3, or the moonquakes may occur within a planar or linear zone of larger dimensions.

The b-values, or slopes, of the cumulative amplitude distributions for the swarms discussed are in the range 2.1 to 2.4, which is near the average value of 2 measured for the larger, periodic moonquakes. (See the section entitled "Statistics of Long-Period Events.")

An unusual swarm began on April 14 with recorded events occurring at a nearly constant rate of 12 per day as the average amplitude of the signals increased with time for a period of approximately 2 days. On April 17, after a 9-hr break in activity, three large moonquakes occurred, the last being the largest ever recorded. No significant aftershock activity was observed. This sequence of activity is represented in figure 8-11. The largest moonquake, though well recorded by the Apollo 12 and Apollo 14 stations, preceded deployment of the Apollo 15 station, and the exact location therefore remains uncertain. However, by assuming that this large moonquake occurred at a depth of 800 km, as estimated for category A_1 moonquakes, an epicenter of latitude 20° N and longitude 72° E is obtained. This location is approximately 2700 and 2900 km from the Apollo 14 and Apollo 12 sites, respectively. The Richter magnitude of this moonquake is 2 to 3 depending on the method of calculation used. The largest category A_1 moonquake observed to date had a magnitude of approximately 1 to 2. The average swarm moonquake in this sequence was comparable in magnitude to a small to intermediate category A_1 moonquake. The buildup in the amplitude of events during the swarm suggests that they are indeed related. However, large moonquakes are not associated with any of the other swarms observed to date.

Similar swarms are common in volcanic regions of the Earth where they often occur before, during, and after eruptions. Swarms are also observed in areas of geologically recent, but not current, volcanism. Sykes (ref. 8-15) reports that earthquake swarms frequently occur along the crustal zones of midoceanic ridges, which are centers of sea-floor spreading and abundant submarine volcanism. Swarms also precede most of the major volcanic eruptions in the Lesser Antilles (ref. 8-16). They may also be observed in nonvolcanic areas where they are believed to represent minor adjustment of crustal blocks to local stress conditions. Sometimes, a swarm precedes a large tectonic earthquake. Whether related to volcanism or not, all earthquake swarms are thought to be of shallow origin. With such relationships in mind, the data on moonquake swarms and matching moonquakes will be examined with great interest as clues to present lunar tectonism.

Moonquakes and Lunar Tectonism

It now appears certain that seismic-energy release related to lunar tides does occur within the Moon. However, the magnitudes and numbers of these events are small in comparison to the total seismic activity that would be recorded by an equivalent seismic station on Earth. Estimated seismic-energy release from the largest moonquakes ranges between 10^9 and 10^{12} ergs. The total energy released by moonquakes, if the Apollo 12 region is typical of the entire Moon, is approximately 10^{11} to 10^{15} ergs/yr. This value compares with approximately 5×10^{24} ergs/yr for total seismic-energy release within the Earth. Considerable uncertainty exists in this estimate, primarily because of the difficulty of estimating the ranges of natural events. However, the average rate of seismic-energy release within the Moon is clearly much less than that of the Earth. Thus, internal convection currents leading to significant lunar tectonism are probably absent. Further, the absence of conspicuous offset surface features and of compressional features such as folded mountains is evidence against significant lunar tectonic activity, past or present. Presently, the outer shell of the Moon appears to be relatively cold, rigid, and tectonically stable compared to the Earth, except for the minor disruptive influence correlated with lunar tides. However, the presence of moonquake swarms suggests continuing minor adjustment to crustal stresses. The occurrence of deep-focus moonquakes leaves open the possibility of slow convection currents at great depth beneath a rigid outer shell.

Statistics of Long-Period Events

Data on the incidence and coincidence of LP events at the Apollo 14 and Apollo 15 stations illustrate some basic properties of the lunar seismic

environment. The cumulative amplitude curves (fig. 8-10) characterize the size distribution of events. The LP events are clearly a mixture of different source types. Therefore, care was taken in classifying events as moonquakes or impacts on the basis of the seismogram characteristics. As indicated in table 8-IV, almost 80 percent of all detected LP events were classified by the criteria discussed previously, although some of the identifications remain in doubt pending further analysis.

Separate cumulative curves of moonquakes and impacts (fig. 8-10) have different slopes, which indicate that the selection process has separated the events into categories representing different source mechanisms. Representing the curves of figure 8-10 by equations of the form

$$\log n = a - b \log A \tag{8-1}$$

the b-value of moonquake distributions is approximately 2 and, for impact distributions, approximately 1. All curves flatten in the low-amplitude range where events become undetectable because of small size. Further, the curves for impact data have a possible break in slope near the midpoints. This observation may indicate an otherwise undetected effect of mixed source types. The suggestion of a break in slope is especially strong for the Apollo 14 station impact data, which are more numerous. Possibly, the impact data may be contaminated with data from swarms of small moonquakes that are not identified as such. Alternatively, impact data may be a composite of two different meteoroid populations, such as stony meteoroids and cometary meteoroids (ref. 8-17).

From table 8-IV (LP signals only), 26 impacts were detected at the Apollo 14 station only, four impacts were detected at the Apollo 15 station only, and five impacts were detected at both stations. From these data, the maximum ranges at which the impacts were detected at each station can be estimated. Assuming that the events identified as impacts are randomly distributed meteoroid impacts, the ratio of the areas from which impacts are detected by the two stations (A_{14}/A_{15}) must approximately equal the ratio of the number of recorded events, or

$$\frac{A_{14}}{A_{15}} = \frac{r_{14}^2}{r_{15}^2} = \frac{31}{9} \tag{8-2}$$

and

$$\frac{A_{OV}}{\pi r_{14}^2} = \frac{5}{31} \tag{8-3}$$

where A_{OV} is the overlap between the two areas, and r_{14} and r_{15} are the radii of the areas of perceptibility at the Apollo 14 and Apollo 15 stations, respectively. Using the additional fact that the stations are 1095 km apart, equations (8-2) and (8-3) can be solved to give r_{14} = 1362 km and r_{15} = 732 km, respectively. Using the same method for impacts recorded at the Apollo 12 station, r_{12} = 951 km is obtained. Thus, a meteoroid that is barely detectable at the Apollo 14 station at a range of 1362 km will be detected only to ranges of 951 and 732 km at the Apollo 12 and Apollo 15 stations, respectively. The instrument sensitivities at the respective stations are matched to within 5 percent. Thus, the differences in the ranges of detectability must be a consequence of differences in local structure at the three sites. These estimates are subject to considerable uncertainty at present, because of the relatively small number of events available for comparison. However, the method illustrated in this report will eventually lead to accurate estimates as data accumulate.

In contrast with the meteoroid-impact signals, most moonquakes are recorded at all three seismic stations. This fact supports the hypothesis that moonquake focuses are deep within the Moon and, hence, more nearly equidistant from the stations than are randomly distributed meteoroid impacts.

Using amplitude data from seismic signals recorded during the Apollo 14 mission (ref. 8-7), the meteoroid flux was estimated assuming that a distribution of meteoroid masses (individual source-receiver distances being unknown) produces the observed distribution of signal amplitudes. The key to such an analysis is a knowledge of the amplitude fall-off law, or variation of amplitude A with range r. The amplitude-range calibration from 63 to 172 km, then available from artificial impacts prior to Apollo 15, was used in deriving the previous estimate. In that range, the amplitude appears to vary as r^{-1}, which would be appropriate at all ranges for a Moon with constant seismic velocity throughout the interior. From data on the more distant artificial Apollo 15 impacts, the amplitude appears to fall off more rapidly in the range between 188 and 1100 km. This variation will become better known after the artificial impacts of the Apollo 16 and Apollo 17 missions.

Considerations of this sort may increase the flux estimate by an order of magnitude. The lower b-value now obtained for the observed cumulative amplitude curve may also modify the estimate of flux, though by a lesser amount. This assumption follows from relationships expressing the calibration between meteorite mass and seismic amplitude as well as the integration of flux contributions over the surface of the Moon, which both depend on the observed b-value. Therefore, it seems best to postpone a revision of the earlier flux estimate until these factors are better known.

CONCLUSIONS

Natural lunar seismic events detected by the Apollo seismic network are moonquakes and meteoroid impacts. The moonquakes fall into two categories: periodic moonquakes and moonquake swarms. All the moonquakes are small (maximum Richter magnitudes between 1 and 2). With few exceptions, the periodic moonquakes occur at monthly intervals near times of perigee and apogee and show correlations with the longer term (7-month) lunar-gravity variations. The moonquakes originate at not less than 10 different locations. However, a single focal zone accounts for 80 percent of the total seismic energy detected. The epicenter of the active zone has been tentatively located at a point 600 km south-southwest from the Apollo 12 and Apollo 14 stations. The focus is approximately 800 km deep. Each focal zone must be small (less than 10 km in linear dimension). Changes in record character that would imply migration of the focal zone or changes in focal mechanism have not been observed in the records over a period of 20 months. Cumulative strain at each location is inferred. Thus, the moonquakes appear to be releasing internal strain of unknown origin, the release being triggered by tidal stresses. The occurrence of moonquakes at great depths implies that the lunar interior at these depths is rigid enough to support appreciable stress and that maximum stress differences occur at these depths. If the strain released as seismic energy is of thermal origin, strong constraints are placed on acceptable thermal models for the deep lunar interior.

Episodes of frequent small moonquakes, called moonquake swarms, have been observed. The occurrence of such swarms appears to bear no relation to the lunar tidal cycle, although present data are not sufficient to preclude this possibility. The source of moonquake swarms has not been determined.

The average rate of seismic-energy release within the Moon is much less than that of the Earth. Thus, internal convection currents leading to significant lunar tectonism appear to be absent. Presently, the outer shell of the Moon appears to be relatively cold, rigid, and tectonically stable compared to the Earth. However, the occurrence of moonquakes at great depth suggests the possibility of very deep convective motion. Moonquake swarms may be generated within the outer shell of the Moon as a result of continuing minor adjustments to crustal stresses.

Seismic evidence of a lunar crust has been found. In the region of the Apollo 12 and Apollo 14 stations, the thickness of the crust is between 55 and 70 km. The velocity of compressional waves in the crustal rock varies between 6.0 and 7.5 km/sec. This range brackets the velocities expected for the feldspar-rich rocks found at the surface. The transition to the subcrustal material may be gradual, beginning at a depth of 20 to 25 km; or sharp, with a major discontinuity at between 55 and 70 km. In either case, the compressional-wave velocity must reach 9 km/sec at a depth between 55 and 70 km. The past occurrence of large-scale magmatic differentiation, at least in the outer shell of the Moon, is inferred from these results.

REFERENCES

8-1. Latham, Gary; Ewing, Maurice; Press, Frank; Sutton, George; et al.: Passive Seismic Experiment. Sec. 6 of Apollo 11 Preliminary Science Report. NASA SP-214, 1969.

8-2. Latham, Gary; Ewing, Maurice; Press, Frank; Sutton, George; et al.: Apollo 11 Passive Seismic Experiment. Science, vol. 167, no. 3918, Jan. 30, 1970, pp. 455-467.

8-3. Latham, Gary; Ewing, Maurice; Press, Frank; Sutton, George; et al.: Apollo 11 Passive Seismic Experiment. Proceedings of the Apollo 11 Lunar Science Conference, Vol. 3, A. A. Levinson, ed., Pergamon Press (New York), 1970, pp. 2309-2320.

8-4. Latham, Gary; Ewing, Maurice; Press, Frank; Sutton, George; et al.: Passive Seismic Experiment. Sec. 3 of Apollo 12 Preliminary Science Report. NASA SP-235, 1970.

8-5. Latham, Gary; Ewing, Maurice; Press, Frank; Sutton, George; et al.: Seismic Data From Man-Made Impacts on the Moon. Science, vol. 170, no. 3958, Nov. 6, 1970, pp. 620-626.

8-6. Ewing, Maurice; Latham, Gary; Press, Frank; Sutton, George; et al.: Seismology of the Moon and Implications of Internal Structure, Origin, and Evolution. Highlights of Astronomy, D. Reidel Pub. Co. (Dordrecht, Holland), 1971.

8-7. Latham, Gary; Ewing, Maurice; Press, Frank; Sutton, Geroge; et al.: Passive Seismic Experiment. Sec. 6 of Apollo 14 Preliminary Science Report. NASA SP-272, 1971.

8-8. Latham, Gary; Ewing, Maurice; Press, Frank; Sutton, George; et al.: Moonquakes. Science, vol. 174, 1971.

8-9. Kovach, Robert; Watkins, Joel; and Landers, Tom: Active Seismic Experiment. Sec. 7 of Apollo 14 Preliminary Science Report. NASA SP-272, 1971.

8-10. Schreiber, E.; Anderson, O.; Soga, N.; Warren, N.; et al.: Sound Velocity and Compressibility for Lunar Rocks 17 and 46 and for Glass Spheres from the Lunar Soil. Science, vol. 167, no. 3918, Jan. 30, 1970, pp. 732-734.

8-11. Kanamori, H.; Nur, A.; Chung, D.; Wones, D.; et al.: Elastic Wave Velocities of Lunar Samples at High Pressures and Their Geophysical Implications. Science, vol. 167, no. 3918, Jan. 30, 1970, pp. 726-727.

8-12. Scholz, C. H.: The Frequency Magnitude Relation of Microfracturing in Rock and Its Relation to Earthquakes. Seismol. Soc. Amer. Bull., vol. 58, no. 1, 1968, pp. 399-415.

8-13. Warren, Nicholas W.; and Latham, Gary: An Experimental Study of Thermally Induced Microfracturing and Its Relation to Volcanic Seismicity. J. Geophys. Res., vol. 75, no. 23, Aug. 10, 1970, pp. 4455-4464.

8-14. Nakamura, Y.; Veach, C.; and McCauley, B.: Research Rept. ERR-FW-1176, General Dynamics Corp., 1971.

8-15. Sykes, Lynn R.: Earthquakes and Sea-Floor Spreading. J. Geophys. Res., vol. 75, no. 32, Nov. 10, 1970, pp. 6598-6611.

8-16. Robson, G. R.; Barr, K. G.; and Smith, G. W.: Earthquake Series in St. Kitts-Nevis, 1961-62. Nature, vol. 195, no. 4845, Sept. 8, 1962, pp. 972-974.

8-17. Hawkins, Gerald S.: The Meteor Population. NASA CR-51365, 1963.